Silver Nanoparticles Decorated Wide Band Gap MoS 2 Nanosheet: Enhanced Optical and Electrical Properties

Priyanku Gogoi
Gauhati University
Sulochana Deb
debsulochana@gauhati.ac.in

Gauhati University

Research Article

Keywords: Molybdenum disulphide nanosheet, silver nanoparticles, surface plasmon resonance, photoluminescence, Raman spectra

Posted Date: January 15th, 2024

DOI: https://doi.org/10.21203/rs.3.rs-3849483/v1

Additional Declarations: No competing interests reported.

Version of Record: A version of this preprint was published at Plasmonics on March 28th, 2024. See the published version at https://doi.org/10.1007/s11468-024-02253-0.

Abstract

Metal nanoparticles decorated Molybdenum disulphide (MoS_2) nanosheets have received great attention of researchers due to their potential applications in biosensing, optoelectronics, photocatalysis, SERS, etc. Here, we report the enhanced optical and electrical properties of wide band gap MoS_2 nanosheets when decorated with silver nanoparticles (Ag-MoS_2 nanosheets). Field Emission Scanning Electron Spectroscopy (FESEM) images reveal the formation of well-shaped MoS_2 nanosheet-like structures decorated with silver nanowires. MoS_2 nanosheets are 27.9 μm long and 12.9 μm wide and the thickness is in the range of nanometer. X-ray diffraction (XRD) spectra show peaks at 25.46°, 33.79°, 36.28°, and 50.97° corresponding to (111), (100), (102), and (105) crystalline planes for pure MoS_2 and at 47.26° and 78.28° corresponding to the (200) and (311) crystalline planes for silver in Ag- MoS_2 nanosheets respectively. The UV-Vis absorption peak is observed at 340 nm for MoS_2 but gets blue-shifted for Ag-MoS_2 nanosheets. The calculated band gap is found to be 3.05eV for MoS_2 nanosheet, so it falls under the category of wide band gap (2–4 eV) semiconductors which can have potential application in UV photodetection. From the photoluminescence spectra, we have observed enhanced emission for Ag-MoS_2 in the range of 410–470 nm for the excitation wavelength 280 nm. Raman peak intensity of MoS_2 nanosheet has increased significantly when decorated with Ag nanostructure which can have potential SERS application. I-V characteristic of Ag-MoS_2 nanosheets under illumination exhibits negative photoconductivity but is positive for pristine MoS_2 nanosheets.

1. Introduction

In the pursuit of next-generation materials for electronic and optoelectronic applications, two-dimensional materials have emerged as exceptional candidates[1]. Two-dimensional (2D) Transition Metal dichalcogenides (MoS_2, WSe_2, WS_2, $MoSe_2$, $MoTe_2$) have received great attention due to its unique optical, electrical, and mechanical properties[2–4]. Among them, Molybdenum disulfide (MoS_2) nanosheets are the most promising candidates because of their potential applications in optoelectronic devices, catalysis, highly effective sensors, batteries, supercapacitors, water desalination, energy storage and many other fields[5–9]. MoS_2 nanosheet has garnered significant attention owing to its unique properties including mechanical flexibility, and a large surface area, number of layers dependent tunable band gap, etc. Bulk MoS_2 has an indirect band gap small indirect band gap of 1.29 eV but MoS_2 in monolayer form has a direct band gap of about 1.9 eV [4] and this bandgap increases with number of layers [10, 11]. Few layer MoS_2 with band gap in the range of 2–4 eV falls under the category of wide band gap semiconductors[12, 13]. Wide band gap semiconductors have high optical transparency, controllable carrier concentration, and tunable electrical conductivity and can withstand higher temperatures, voltages and frequencies. So, wide band gap MoS_2 can have potential application in UV photodetector and other optoelectronic devices as[14]. However, to fully exploit its potential, researchers are exploring innovative strategies to enhance its optical and electrical properties. In this context, the incorporation of metal nanoparticles into two-dimensional materials has proven to be a promising

avenue for tuning the optical and optoelectronic properties. Decoration of metal nanoparticles such as nanoparticles of gold, silver, platinum and palladium on the surface of the MoS_2 nanosheet enhances its properties due to the synergistic advantages of MoS_2 and the plasmonic capabilities of metal nanoparticles [15–19]. Plasmonic nanoparticles can enhance the absorption and scattering of light can also improve carrier generation and collection in MoS_2[20–22].

There are different methods to fabricate MoS_2 nanosheets, including mechanical cleavage, solvothermal synthesis methods, chemical vapor deposition (CVD), exfoliation methods, and solvent-based sonication [23–25]. Among all these method, hydrothermal method is simple for facile synthesis of MoS_2 nanosheets.

We report here simple hydrothermal method for the synthesis of well-shaped Molybdenum disulfide (MoS_2) nanosheet with wide band gap and silver (Ag) nanoparticles decorated MoS_2 nanosheet.

The primary objective of this study is to investigate the impact of silver nanoparticles on the optical and electrical properties of wide band gap MoS2 nanosheets. By strategically decorating MoS2 with silver nanoparticles, we aim to enhance light-matter interactions. Through a systematic exploration of the underlying mechanisms, this research seeks to contribute to the fundamental understanding of the synergies between wide band gap MoS2 and silver nanoparticles for its application as optoelectronic device.

2. Experimental

2.1 Material used

To prepare the MoS_2 nanosheet, the materials used are Ammonium heptamolybdate tetrahydrate $(NH_4)_6Mo_7O_{24}.4H_2O$ citric acid ($C_6H_8O_7$), Ammonia water solution, and Thiourea (CH_4N_2S). For the synthesis of the Ag-MoS_2 nanosheet, Silver Nitrate ($AgNO_3$) is used. Ammonium heptamolybdate tetrahydrate $(NH_4)_6Mo_7O_{24}.4H_2O$ and Silver Nitrate ($AgNO_3$) are acquired from Sigma-Aldrich Company and 99.9% pure, citric acid ($C_6H_8O_7$), Ammonia water solution and Thiourea (CH_4N_2S) are obtained from E -Mark Company and 99.9% pure are used.

2.2 Method of Synthesis and Characterization

For the synthesis of MoS_2 nanosheets, 1.7 mmol of ammonium heptamolybdate tetrahydrate $(NH_4)_6Mo_7O_{24}.4H_2O$ and 3.6 mmol citric acid ($C_6H_8O_7$) are mixed at 90°C with constant stirring for 60 minutes. To achieve a pH of 4.90, the ammonia water solution is added dropwise. 17.08 m mol thiourea (CH_4N_2S) is added drop-by-drop to the solution which is continuously stirred for 30 min at 60°C. The color of the solution changes to pale blue. The mixture is then put into a Teflon autoclave for two hours at 120°C.

To prepare Ag-MoS_2 nanosheet 20mM and 25mM Silver Nitrate ($AgNO_3$) in 10 ml of water ($AgNO_3$) is added dropwise to the MoS_2 solution at a temperature of 60°C and stirred for 45 minutes, Now the solution is cloudy and covered with precipitate.

3. Characterization

The morphology of the three hydrothermally prepared samples MoS_2 nanosheet, 20 mM Ag- MoS2 nanosheet and 25 mM Ag- MoS2 are studied using Field Emission Scanning Electron microscopy (FESEM) images collected by FESEM (ZEISS). Structural properties are characterized by X-ray diffraction (XRD) data collected by EMPYREAN, PANalytical with Cu-Kα (0.15418 nm) radiation. For optical properties, UV–Vis optical absorption spectra are recorded by CARY-300 spectrophotometer, and Photoluminescence (PL) spectra are taken by JASCO FP- 8300 Spectrofluorometer. TGA analysis is done by Mettler Toledo, TGA/DSC-1, star System. Raman spectrometer is recorded by Horiba Jobin Yvon LabRam HR. The electrical properties of the three samples are measured by recording data for current–voltage (I-V) characteristics and photocurrent using Keithly 2400 source meter.

4. Result and discussion

4.1 Morphological study and elemental analysis

The surface morphology of pristine MoS_2 nanosheet, 20 mM Ag- MoS_2 nanosheet, and 25 mM Ag- MoS_2 is studied using a field emission scanning electron microscope (FESEM). The FESEM images are shown in Fig. 1 (a), (b), and (c). In the FESEM pictures, it is observed that the nanosheets have thickness in the nanometer range and length and breadth in the 25–45μm range. The nanosheets are seen to be piled together in various locations in the FESEM pictures shown in Fig. 1 (a). Silver nanostructures with erratic shapes are seen above the MoS_2 nanosheets in Figs. 1(b) and 1(c).

The electron dispersion X-ray (EDAX) of the three samples is shown in Fig. 2(a), (b), and (c). In addition to the elements Mo and S, the findings of the EDAX spectrum analysis reveal a rather high oxygen concentration. This is because MoS_2 nanosheet has a high surface energy that quickly interacts with water molecules and forms bonds with oxygen [26].

4.2 Structural analyses

Using the X-ray diffractometer, the phase identification and associated microstructural investigations are carried out (EMPYREAN, PANalytical). At an accelerating voltage of 45 kV and an anode current of 40 mA, the diffractometer is in operation. Cu K radiation with an X-ray wavelength of 0.15406 nm is permitted to impact the samples. The XRD patterns are captured at a step size of 0.026 in the 2 range of 10°-80^0. According to Fig. 3, the characteristic peak of MoS_2 prepared at 120°C for an autoclave is seen at 36.28°, 50.97°, and 72.04°, which correspond to (102), (105), and (203) planes (JCPDS 00-037-1492). Also,

according to JCPDS 00-001-1164, a distinctive silver peak can be seen in silver-decorated MoS_2 at 47.26° and 78.28°, which correspond to the (200) and (311) planes, respectively (JCPDS 00-001-1164). This indicates that the Ag nanoparticles are decorated on the MoS_2 nanosheet.

4.3 Optical Properties

4.3.1 UV–Visible absorption spectra

The UV–Visible absorption spectra are shown in Fig. 4(a). The transition from the valence band to the conduction band is characterized by a distinctive absorption peak at about 340 nm. The K point of the Brillouin zone causes an additional board peak to be seen between 600 to 800 nm, which is connected to the excitonic A transition [27]. The absorption peak is blue-shifted with the increase in silver nitrate concentration. The optical band gap is determined by using the Tauc plot relation Fig. 4(b) and is given by,

$(\alpha hv)^n = B(hv - E_g)$

where α is absorbance, (hv) is the incoming radiation's energy, B is the proportionality constant, h = 1.38 $\times 10^{23}$ is the Plank's constant, and E_g is the material's band gap. In the Tauc plot relation, for indirect band gap material value of n = 1/2. The band gap for indirect transition may be determined from the extrapolation of the linear section of the curves to the x-axis for $(\alpha(v)hv)^{1/2} = 0$. The calculated band gap is found to be 3.05eV, 3.16 eV, and 3.23eV for MoS_2 nanosheet, 20 mM Ag- MoS_2 nanosheet and 25 mM Ag- MoS_2 respectively. The increase in band gap of the nanocomposite may be due to the quantum confinement effect. The calculated band gap indicates that the samples fall under the category of wide-bandgap semiconductors [28, 29].

4.3.4 Photoluminescence (PL) spectra

The room temperature photoluminescence (PL) spectra of the MoS_2 nanosheet, 20 mM Ag- MoS_2 nanosheet, and 25 mM Ag- MoS_2 nanoparticles are shown in Fig. 7. The PL spectra are recorded by the F-7000 FL Spectrophotometer with an excitation wavelength of 280 nm. From the figure, it is seen that for pristine MoS_2 there is a board emission spectrum center around 413nm, the band gap calculated from this peak is 3.0 eV which is slightly less than the indirect bandgap calculated from UV-vis data. For silver-embedded MoS_2 there are two peaks around 398nm (3.115eV) which is somewhat less than the bandgap estimated from the UV-vis data and a peak at 469nm is mainly due to radiative recombination of bound excitations from traps and defects levels[30]. The enhancement of the PL intensity after embedding silver may be due to the surface plasmonic effect [31].

4.4 Raman Spectroscopy

Figure 8 displays the Raman spectrum of as-prepared MoS_2 and Ag-MoS_2 nanocomposites. Raman spectra of MoS_2 reveal three distinct Raman peaks that can be attributed to the E_{1g}, A_1, and E^1_{2g} vibrational modes of the S atoms with respect to the Mo atom, respectively. Also, a typical peak of 454 cm^{-1}, in the spectrum is designated as 2LA (M)[32]. The Ag-MoS_2 nanocomposite also displays similar Raman peaks of MoS2, which suggests that the reduction process had little to no impact on the chemical composition of the nanosheets[33]. Additionally, the Raman peak intensity is noticeably increased which indicates that the Ag Nanoparticle decorated structure has potential in SERS application [34].

4.5 Thermogravimetric analysis

Thermogravimetric analyses (TGA) were used to investigate the thermal stability of MoS_2 and silver-decorated MoS_2 nanocomposite in an N_2 environment. The results are shown in Fig. 9. Around 100°C, MoS_2 experiences an initial weight loss that is ascribed to water molecules that have been adsorbed. Additionally, MoS_2 exhibits weight loss at temperatures near 400°C, which may be due to MoS_2 being oxidized into MoO_3[32, 35]. Future no degradation is observed for temperatures from 500°C to 700°C. On the other hand, for silver decorated MoS_2 the TGA curve shows that the sample lost the majority of its weight between 200 and 300°C. Above 300°C, there is hardly any dominant weight loss till 700°C. It can be generally attributed to the evaporation of organic substances[36].

4.6 Electrical properties

Electrical properties of MoS_2 nanosheet, 20 mM Ag- MoS_2 nanosheet and 25 mM Ag- MoS_2 are measured through I-V characteristics curves under dark as well as under illumination of 365nm and 440nm. At room temperature (300K), the I-V characteristic is determined by two probe method using two fine copper wires into a tiny film region using silver paste. The I-V characteristics are shown in Fig. 10(a), (b), (c) it is observed that the photocurrent increases slightly in pristine MoS_2 and 20mM silver-decorated MoS_2 but we can observe a gradual decrease in photocurrent for 25mM silver-decorated MoS_2. Decorating silver nanoparticles over MoS_2 nanosheets led to increase in numbers of defects and trap levels. These Shallow traps that function as donor or acceptor states are thought to be the cause of negative photoconductivity. The ratio between the rates of recombination and generation is the main qualitative factor contributing to negative photoconductivity [37, 38].

Conclusion

We have successfully synthesized well shaped MoS_2 nanosheet and silver-decorated MoS_2 nanosheet using a simple hydrothermal process within 3 hours. Characterization of these samples is carried out using SEM, XRD, UV-Vis, and PL spectroscopy. When the concentration of silver varied, a noticeable effect on MoS_2 is noticed. The creation of stacked MoS_2 nanosheets containing silver particles is verified by SEM pictures. The energy-dispersive X-ray analyzer confirms the produced MoS_2 constituent

composition. Ag peaks at 47.26° and 78.28° correlate to (200) and (311) planes with an average crystallographic size of 55.23 nm, whereas MoS_2 characteristics peaks at 36.28°, 50.97°, and 72.04° correspond to (102), (105) and (203) planes. The straight transition from the deep valence band to the conduction band causes the UV-Vis absorption spectra to exhibit significant absorption at about 340 nm. PL measurements depict that the MoS_2 with silver nanostructure exhibits emission peaks in the PL spectrum at 469 nm, suggesting emission from the silver also indicated that the intensity of the emission spectra increases with the addition of silver due to the surface resonance effect. The investigation of electric properties using I-V characteristics under dark and illumination at 300 K reveals that conductivity diminishes as silver content increases showing negative photoconductivity.

Declarations

Acknowledgments

The authors express their deep sense of gratitude to SAIF, Gauhati University, for SEM and XRD measurement, Prof. D. Sarkar, Dept. of Physics, Gauhati University for electrical measurements, and Mr. Rejaul Hoque, Department of Chemistry for PL measurement.

Ethical Approval: Not applicable

Competing interest: *"The authors have no relevant financial or non-financial interests to disclose."*

Author's contribution: "All authors contributed to the study conception and design. Synthesis, characterization of the samples and all data analyses are done by Sulochana Deb and Priyanku Gogoi. The first draft of the manuscript is written by Sulochana Deb and all authors commented, reviewed and agreed on the final manuscript".

Funding: "The authors acknowledge the financial support from UGC-DAE CSR through a Collaborative Research Scheme (CRS) project number CRS/2022-23/01/709."

Availability of data and materials: *"The datasets generated during and/or analyzed during the current study are available from the corresponding author on reasonable request."*

References

1. Tavakkoli M, Soofi H, Sheibaei V (2023) Hybrid MoS2-Plamonic Absorber Covering the Whole Visible Spectrum: Application to Design Transistor Like Photodetectors. Plasmonics 1–6. https://doi.org/10.1007/S11468-023-01958-Y/METRICS
2. Wu X, Sun M, Yu H et al (2023) Unraveling the unique response behaviors of ultrathin transition metal dichalcogenides to external excitations. Nano Energy 115:108721. https://doi.org/10.1016/j.nanoen.2023.108721

3. Joseph S, Mohan J, Lakshmy S et al (2023) A review of the synthesis, properties, and applications of 2D transition metal dichalcogenides and their heterostructures. Mater Chem Phys 297:127332. https://doi.org/10.1016/j.matchemphys.2023.127332
4. Chen K, Pan J, Yin W et al (2023) Flexible electronics based on one-dimensional inorganic semiconductor nanowires and two-dimensional transition metal dichalcogenides. Chin Chem Lett 34:108226. https://doi.org/10.1016/j.cclet.2023.108226
5. Karim SS, Sudais A, Shah MS et al (2023) A contemplating review on different synthesis methods of 2D-Molybdenum disulfide (MoS2) nanosheets. Fuel 351:128923. https://doi.org/10.1016/j.fuel.2023.128923
6. Ghaleghafı E, Rahmani MB (2023) Characterization and room temperature ammonia sensing application of hydrothermally synthesized MoS2/RGO nanocomposites. Diam Relat Mater 137:110174. https://doi.org/10.1016/j.diamond.2023.110174
7. Kanjana N, Maiaugree W, Lunnoo T et al (2023) One-step hydrothermal synthesis and electrocatalytic properties of MoS2/activated carbon composite derived from shallots. J Appl Electrochem 53:2311–2320. https://doi.org/10.1007/s10800-023-01921-z
8. Hosseini SM, Safarifard V (2024) MoS2@MOF composites: Design strategies and photocatalytic applications. Mater Sci Semicond Process 169:107892. https://doi.org/10.1016/j.mssp.2023.107892
9. Tavakkoli M, Soofı H, Sheibaei V (2023) Hybrid MoS2-Plamonic Absorber Covering the Whole Visible Spectrum: Application to Design Transistor Like Photodetectors. https://doi.org/10.1007/s11468-023-01958-y. Plasmonics
10. Bafekry A, Faraji M, Abdollahzadeh Ziabari A et al (2021) A van der Waals heterostructure of MoS2/MoSi2N4: a first-principles study. New J Chem 45:8291–8296. https://doi.org/10.1039/D1NJ00344E
11. Chen K, Pan J, Yin W et al (2023) Flexible electronics based on one-dimensional inorganic semiconductor nanowires and two-dimensional transition metal dichalcogenides. Chin Chem Lett 34:108226. https://doi.org/10.1016/J.CCLET.2023.108226
12. Mahdavi M, Kimiagar S, Abrinaei F (2020) Preparation of Few-Layered Wide Bandgap MoS2 with Nanometer Lateral Dimensions by Applying Laser Irradiation. Cryst (Basel) 10:164. https://doi.org/10.3390/cryst10030164
13. Sulochana Deb JS (2021) Proceedings of 28th National Conference on Condensed Matter Physics. In: Nair Ranjith G, Seban Lalu, Ningthoukhongjam Pujita (eds) Springer Proceedings in Physics. Springer, New work, pp 1–9
14. Zhou X, Lu Z, Zhang L, Ke Q (2023) Wide-bandgap all-inorganic lead-free perovskites for ultraviolet photodetectors. Nano Energy 117:108908. https://doi.org/10.1016/j.nanoen.2023.108908
15. Singh J, Soni RK, Nguyen DD et al (2023) Enhanced photocatalytic and SERS performance of Ag nanoparticles functionalized MoS2 nanoflakes. Chemosphere 339:139735. https://doi.org/10.1016/j.chemosphere.2023.139735

16. Li M, Kuo Y-C, Chu X et al (2021) MoS2 nanoflower incorporated with Au/Pt nanoparticles for highly efficient hydrogen evolution reaction. Emergent Mater 4:579–587. https://doi.org/10.1007/s42247-020-00154-6
17. Gholipur R, Taha NA, Afrouzeh K (2023) Synthesis and identification of structural, optical, electrical, magnetic, photocatalytic, and electrochemical properties of novel Au/MoS2@(NiFe2O4)x nanocomposites. Sens Actuators A Phys 362:114645. https://doi.org/10.1016/j.sna.2023.114645
18. Nie S, He W, Xu Y et al (2023) Molybdenum disulfide@nickel phyllosilicate hybrid for improving the flame retardancy and wear resistance of epoxy composites. Front Chem Sci Eng 17:2114–2126. https://doi.org/10.1007/s11705-023-2357-1
19. Liu W, Zhong W, Bai G et al (2024) Modulation of magnetism in transition-metal-doped monolayer MoS2 by strain engineering. Mater Chem Phys 311:128523. https://doi.org/10.1016/j.matchemphys.2023.128523
20. Selamneni V, Raghavan H, Hazra A, Sahatiya P (2021) MoS $_2$ /Paper Decorated with Metal Nanoparticles (Au, Pt, and Pd) Based Plasmonic-Enhanced Broadband (Visible-NIR) Flexible Photodetectors. Adv Mater Interfaces 8. https://doi.org/10.1002/admi.202001988
21. Baby M, Kumar KR (2020) Enhanced luminescence of silver nanoparticles decorated on hydrothermally synthesized exfoliated MoS2 nanosheets. Emergent Mater 3:203–211. https://doi.org/10.1007/s42247-019-00066-0
22. Oumekloul Z, Zeng S, Achaoui Y et al (2021) Multi-layer MoS2-Based Plasmonic Gold Nanowires at Near-Perfect Absorption for Energy Harvesting. Plasmonics 16:1613–1621. https://doi.org/10.1007/s11468-021-01405-w
23. Zhou S, Li P, Ji H et al (2023) Scalable synthesis of few-layered MoS2/C sandwiched nanocomposites via ionic crystal (NH4)2MoS4 assisted ball-milling method and their enhanced high-rate lithium storage property. Adv Powder Technol 34:104060. https://doi.org/10.1016/j.apt.2023.104060
24. Tian D, Kang L, Zhang Z et al (2023) Controlled synthesis of continuous MoS2 films via space-confined vapor deposition. Chem Phys 571:111923. https://doi.org/10.1016/j.chemphys.2023.111923
25. Tian Z, Guo H, Liu W et al (2022) Facile exfoliation of MoS2 powders into nanosheets with excellent fluorescence quenching performance of perovskite. Optik (Stuttg) 251:168480. https://doi.org/10.1016/j.ijleo.2021.168480
26. Hasmin HF, Imawan C, Fauzia V (2021) The Role of Temperature in the Hydrothermal Synthesis on the Structural and Morphological Properties of MoS $_2$. J Phys Conf Ser 1951:012014. https://doi.org/10.1088/1742-6596/1951/1/012014
27. Lukianov MY, Rubekina AA, Bondareva JV et al (2023) Photoluminescence of Two-Dimensional MoS2 Nanosheets Produced by Liquid Exfoliation. Nanomaterials 13:1982. https://doi.org/10.3390/nano13131982

28. Li Z, Yan T, Fang X (2023) Low-dimensional wide-bandgap semiconductors for UV photodetectors. Nat Rev Mater 8:587–603. https://doi.org/10.1038/s41578-023-00583-9
29. Kalra A, Muazzam UU, Muralidharan R et al (2022) The road ahead for ultrawide bandgap solar-blind UV photodetectors. J Appl Phys 131. https://doi.org/10.1063/5.0082348
30. Pham VH, Kim K-H, Jung D-W et al (2013) Liquid phase co-exfoliated MoS2–graphene composites as anode materials for lithium ion batteries. J Power Sources 244:280–286. https://doi.org/10.1016/j.jpowsour.2013.01.053
31. Nakaji K, Li H, Kiba T et al (2012) Plasmonic enhancements of photoluminescence in hybrid Si nanostructures with Au fabricated by fully top-down lithography. Nanoscale Res Lett 7:629. https://doi.org/10.1186/1556-276X-7-629
32. Bahuguna A, Kumar S, Sharma V et al (2017) Nanocomposite of MoS_2 -RGO as Facile, Heterogeneous, Recyclable, and Highly Efficient Green Catalyst for One-Pot Synthesis of Indole Alkaloids. ACS Sustain Chem Eng 5:8551–8567. https://doi.org/10.1021/acssuschemeng.7b00648
33. Chuang M-K, Yang S-S, Chen F-C (2015) Metal Nanoparticle-Decorated Two-Dimensional Molybdenum Sulfide for Plasmonic-Enhanced Polymer Photovoltaic Devices. Materials 8:5414–5425. https://doi.org/10.3390/ma8085252
34. Li J, Zhang W, Lei H, Li B (2018) Ag nanowire/nanoparticle-decorated MoS2 monolayers for surface-enhanced Raman scattering applications. Nano Res 11:2181–2189. https://doi.org/10.1007/s12274-017-1836-4
35. Qiu H, Zheng H, Jin Y et al (2020) Dopamine-derived N-doped carbon-encapsulated MoS2 microspheres as a high-performance anode for sodium-ion batteries. Ionics (Kiel) 26:5543–5551. https://doi.org/10.1007/s11581-020-03734-y
36. Majeed Khan MA, Kumar S, Ahamed M et al (2011) Structural and thermal studies of silver nanoparticles and electrical transport study of their thin films. Nanoscale Res Lett 6:434. https://doi.org/10.1186/1556-276X-6-434
37. Xiao X, Li J, Wu J et al (2019) Negative photoconductivity observed in polycrystalline monolayer molybdenum disulfide prepared by chemical vapor deposition. Appl Phys A 125:765. https://doi.org/10.1007/s00339-019-3054-2
38. de Paiva AB, Correr GI, Ugucioni JC et al (2021) On the photoconductivity behavior of emeraldine-salt polyaniline films. Synth Met 281:116915. https://doi.org/10.1016/j.synthmet.2021.116915

Figures

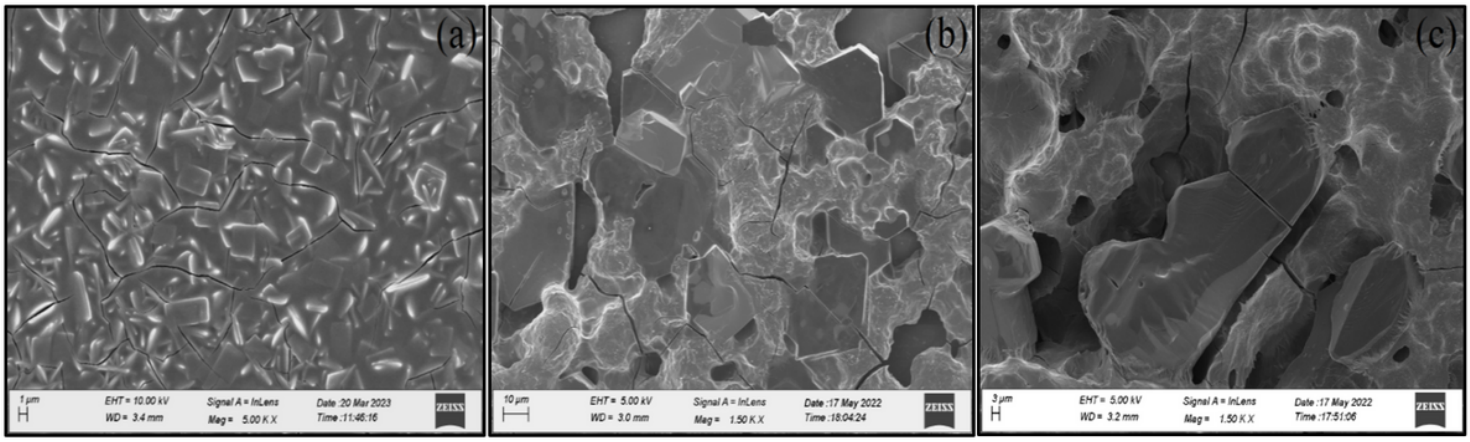

Figure 1

FESEM images of **(a)** Pristine MoS_2 **(b)** 20mM Ag-MoS_2 and **(c)** 25mM Ag-MoS_2

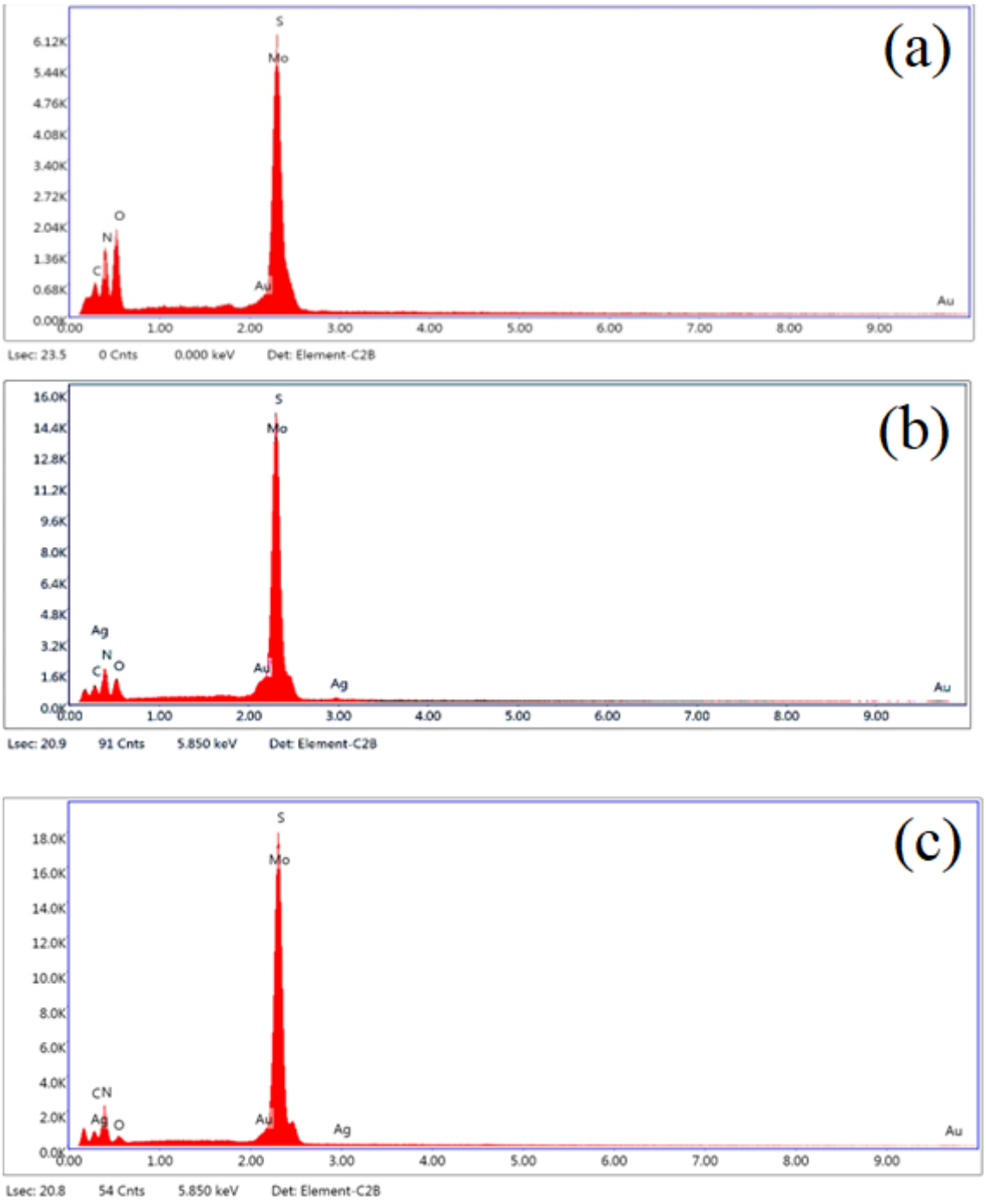

Figure 2

Electron dispersion X-ray (EDAX) of the three samples is shown in the figures. **(a)** pristine MoS_2. **(b)** 20mM Ag-MoS_2 **(c)** 25mM Ag-MoS_2

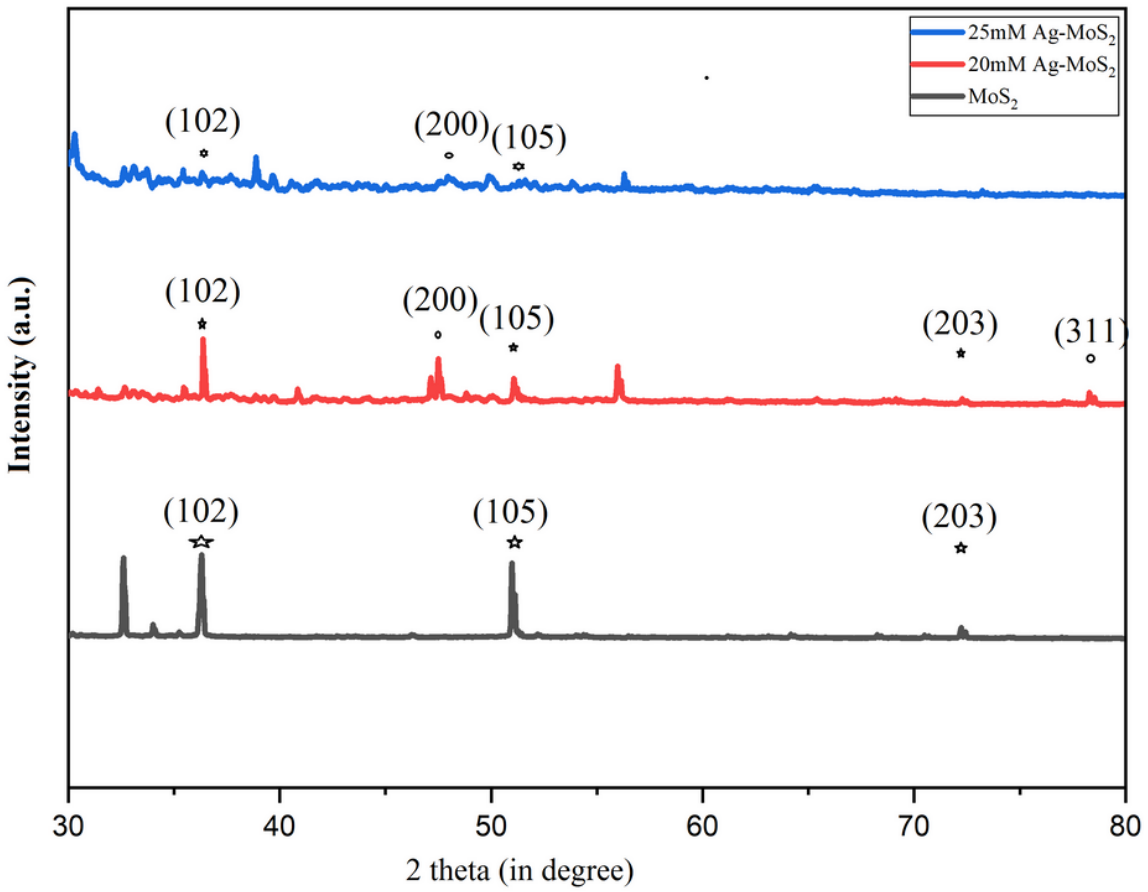

Figure 3

Shows the Powder X-Ray diffraction of the pristine MoS_2 nanosheet, 20 mM Ag- MoS_2 nanosheet, and 25 mM Ag- MoS_2.

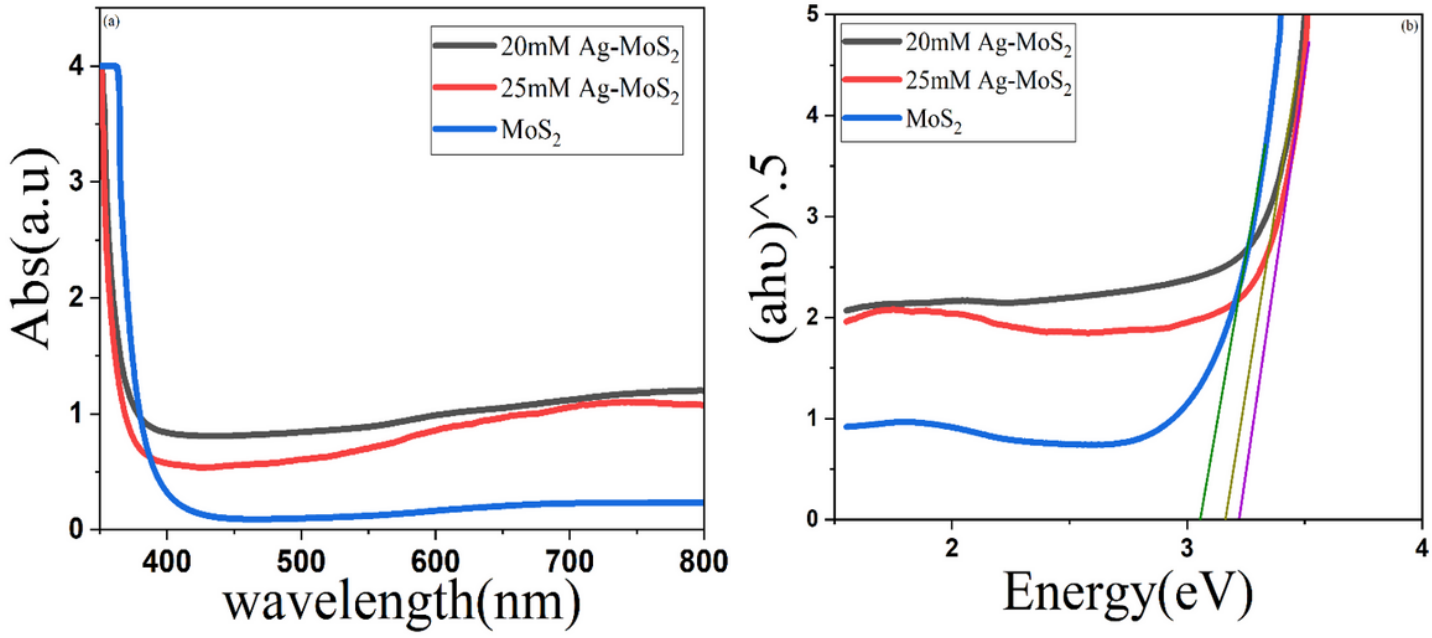

Figure 4

(a) UV-Visible spectrum of pure MoS_2 (blue), 20mM Ag-MoS_2 (black) and 25mM Ag-MoS_2 (red). **(b)** shows the tauc plot for pure MoS_2 (blue), 20mM Ag-MoS_2 (black) and 25mM Ag-MoS_2 (red).

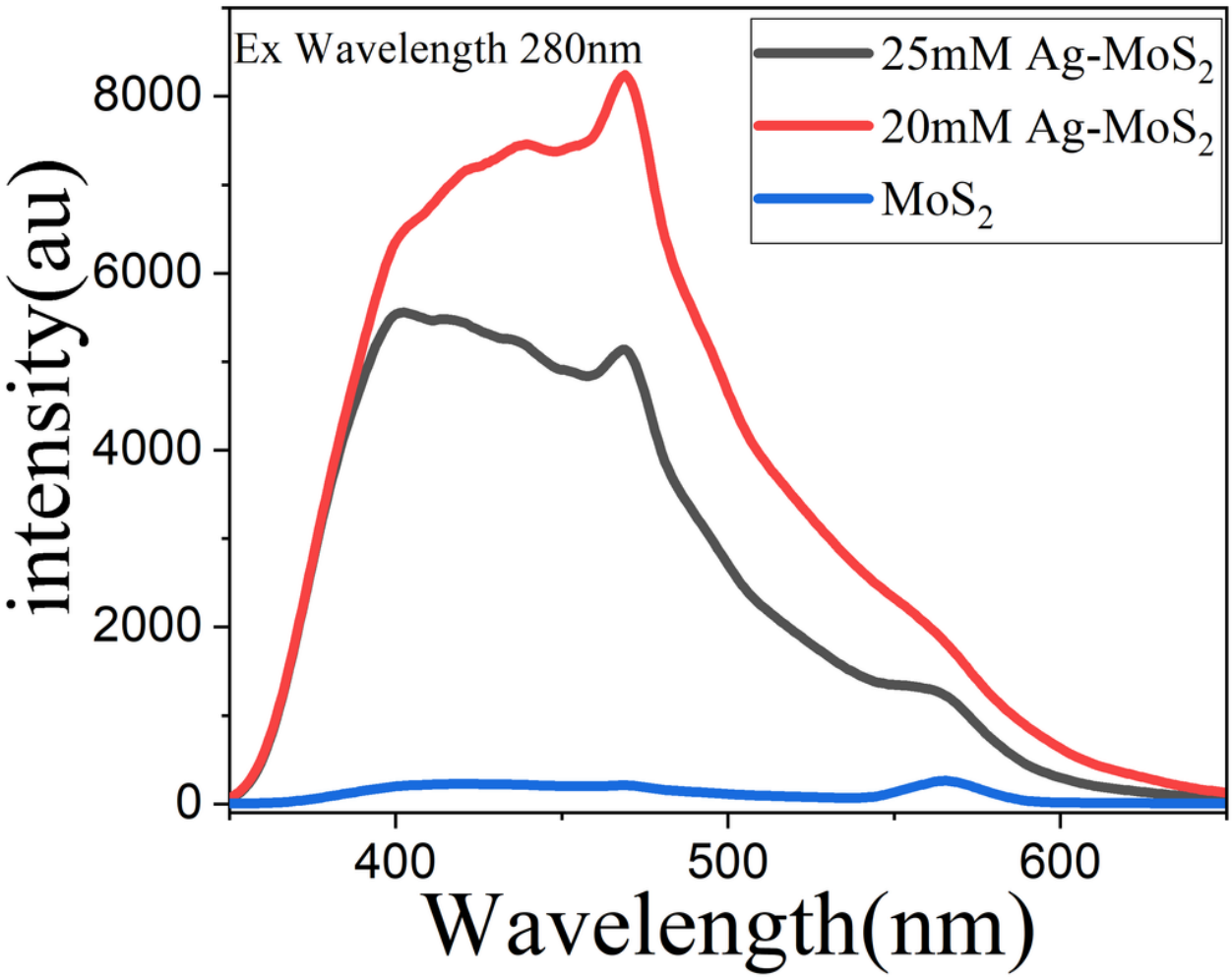

Figure 5

Shows the photoluminescence spectrum of pure MoS_2 (blue), 20mM Ag-MoS_2 (red) and 25mM Ag-MoS_2 (black) with excitation wavelength of 280nm

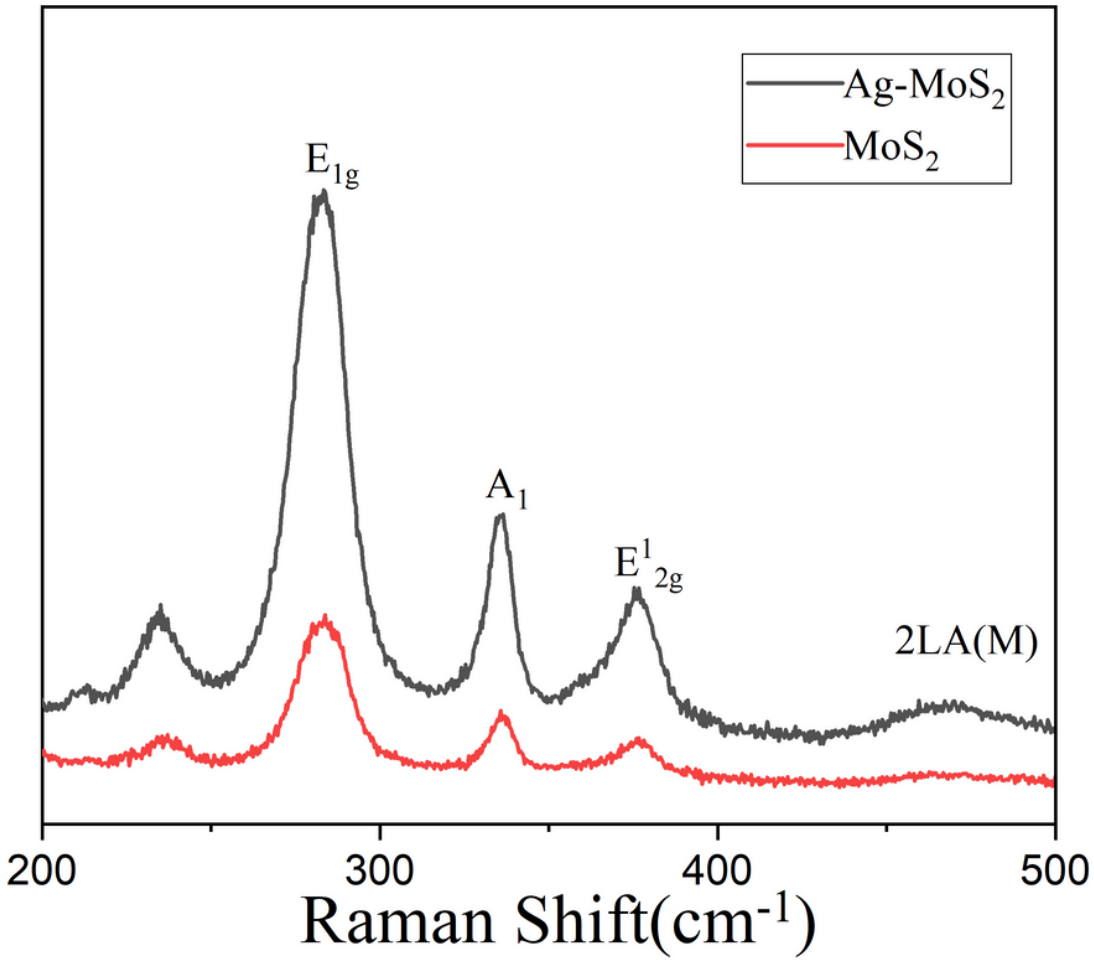

Figure 6

Shows the Raman spectroscopy of the pure MoS_2 nanosheets(red) and Ag-doped MoS_2 nanosheets(black) for 663nm laser radiation.

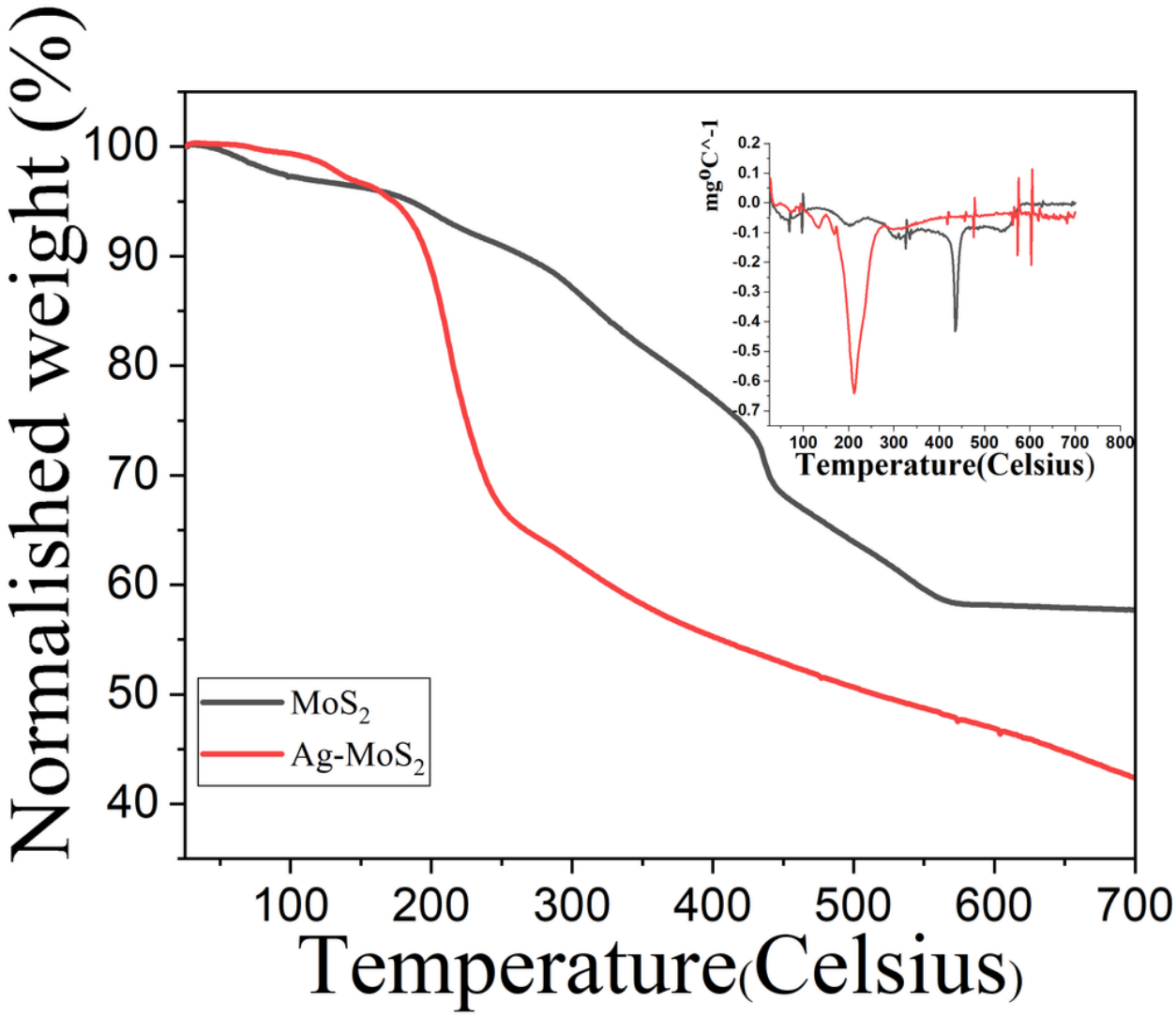

Figure 7

Shows the Thermogravimetric analysis of pure MoS_2 nanosheets(black) and Ag dopped MoS_2 nanosheets (red) in N_2 environment. The inset picture shows the 1^{st} derivative of weight with respect to temperature.

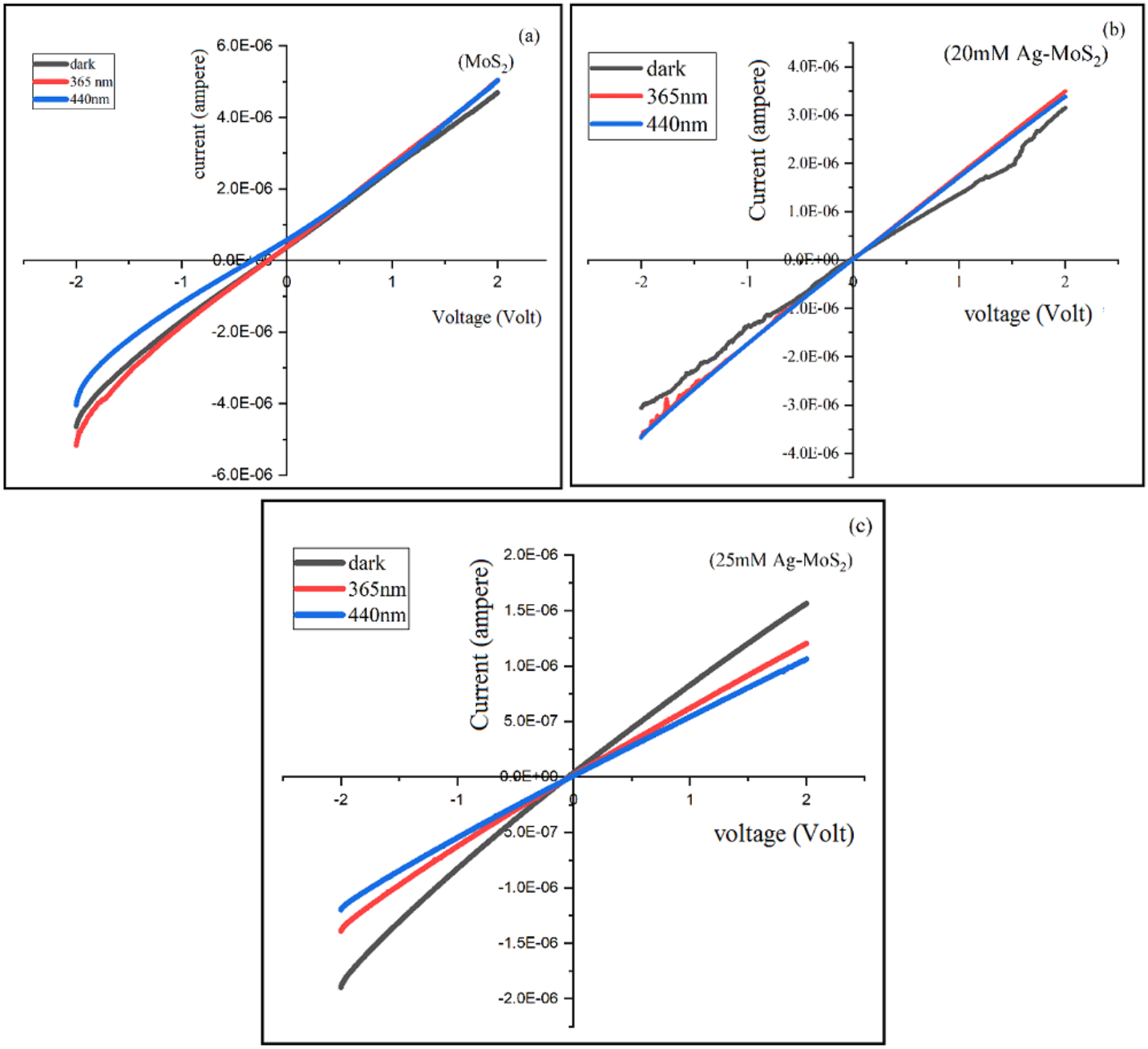

Figure 8

Shows the IV characterization of the as-synthesis samples under different illumination. **(a)** shows the I-V Characteristic of pure MoS_2 whereas **(b)** shows the IV characteristic of 20mM Ag-MoS_2 and **(c)** 25mM Ag-MoS_2.